

# Changes in crystallographic orientation of thin foils of palladium and palladium alloys after the absorption of hydrogen

A.L. Cabrera<sup>1</sup>, E. Morales-Leal

*Facultad de Física, Pontificia Universidad Católica de Chile, Casilla 306,  
Santiago 22, Chile*

J. Hasen and Ivan K. Schuller

*Department of Physics, University of California, San Diego, La Jolla,  
CA 92093-0319, USA*

Received 4 May 1994; accepted 15 September 1994

The adsorption/absorption of hydrogen at room temperature by palladium, 16% silver–palladium and 5% ruthenium–palladium foils was studied using thermal desorption spectroscopy. Hydrogen readily diffused in the palladium and desorbed as one broad peak at about 650 K. Hydrogen also diffuses in the 16% silver–palladium foil and in the 5% ruthenium–palladium foil but with a smaller diffusion constant. Two hydrogen desorption peaks are observed for the Ru–Pd and Ag–Pd alloys, at 440 and around 650 K. The first hydrogen desorption peak is regarded as hydrogen desorbing from the surface sites while the second peak is regarded as hydrogen diffusing from the subsurface sites. The desorption order for surface hydrogen corresponds to  $n = 2$  while the diffused hydrogen desorbs with a fractional order of  $n = 1.25$ . The crystallographic orientation of the foils determined by X-ray diffraction shows a preferential (1, 1, 0) orientation along the direction of rolling of the foils before hydrogen absorption. This preferential orientation is destroyed after hydrogen adsorption for Pd and Pd–Ag but unaltered for the Pd–Ru alloy. This preferential orientation of the foils might have significant implications in membrane fabrication, since the absorption of hydrogen by Pd is very dependent on surface orientation.

**Keywords:** hydrogen absorption; palladium membranes; hydrogen diffusion; hydrogen storage

## 1. Introduction

The interaction of hydrogen with palladium (Pd) is a subject of current interest due to the potentially important technological applications in the area of metallic membranes. Gryaznov [1,2] pioneered work on hydrogen diffusion through thin-

<sup>1</sup> To whom correspondence should be addressed.

walled pure metal membranes for catalytic applications. The facile permeation of hydrogen through palladium and palladium alloys suggests a number of applications in some chemical processes. This knowledge can be incorporated into the design of more efficient reactors [3] for several hydrogenation or dehydrogenation reactions. Nevertheless, the feasibility of an industrial application (at large scale) relies on reducing the cost of the reactor, since a reactor made of Pd would be extremely expensive. Understanding the interaction of hydrogen with Pd may lead to the discovery of other alloys which incorporate inexpensive metals yet provide easy diffusion of hydrogen through the alloy.

The *absorption* of hydrogen by Pd was tentatively explained by Lagos [4–6] as a process mediated by subsurface bonding of hydrogen. According to Lagos' calculations, hydrogen would prefer to bind to subsurface sites rather than surface sites in Pd based on the energy required for the binding. The preferential absorption of hydrogen by these subsurface sites would facilitate hydrogen diffusion into the bulk of the metal. Experimental work reporting subsurface adsorption of hydrogen in other metals, e.g. Nb [7] and Cu [8], have also been published. Thus, this effect does not appear to be unique to the hydrogen–Pd system. Understanding how hydrogen atoms find their way to penetrate below the surface in Pd is important, to be able to modify less expensive metals and alloys for hydrogen storage purposes.

In this model, a subsurface site for hydrogen is an interstitial site below the first layer of metal atoms. In the case that the surface structure of the metal is not closely compacted, like Pd(1, 1, 0), the definition of subsurface site becomes ambiguous. In fact, Rieder and co-workers [9] defined subsurface site in Pd(1, 1, 0) as an interstitial site between the first and second metal layers.

The surface structure of Pd(1, 1, 0) is represented in fig. 1 using a computer program developed by Van Hove and Hermann [10]. In this program, hydrogen and Pd atoms are drawn using their relative covalent radii. A hydrogen atom represented by the smaller dark circle is sitting at the “subsurface” site defined by Rieder and co-workers. Sites on top of the first Pd layer (site 1 in fig. 1) and between the first and second Pd layer (site 2) are surface chemisorption sites, while the interstitial site 3 is a real subsurface site. Equivalent interstitial bulk sites to site 4 in the same figure are sites for hydrogen bulk diffusion. The purpose of our work is to determine the binding energy for hydrogen at site 3 in fig. 1 using thermal desorption spectroscopy (TDS) and correlate these energies with crystallographic information of the Pd or Pd alloy foils.

There is a significant amount of prior experimental work in the H–Pd system which deals with surface interaction only [11–15], a weakly bound subsurface state [11,16,17] on single crystals of Pd, and bulk hydrogen diffusion in Pd [18–21]. In addition, there is also experimental work to determine surface cleanliness of Pd from CO adsorption [22–24].

Taking advantage of our experience in hydrogen adsorption by transition metal foils [25,26], we decided to perform thermal desorption experiments of hydrogen from Pd, Ag–Pd and Ru–Pd foils. The aim of these studies was to obtain a quick

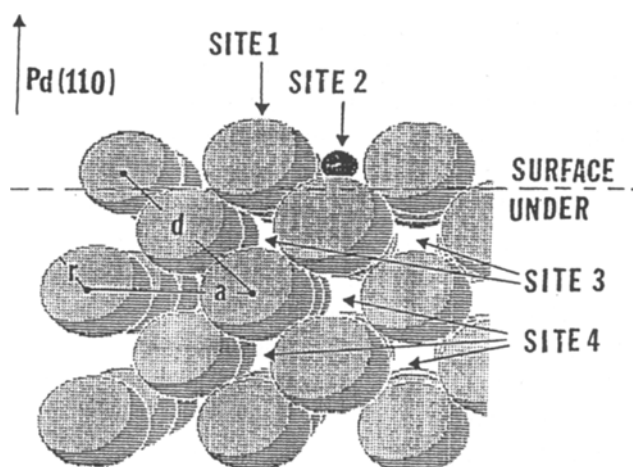


Fig. 1. Picture of the surface of an ideal Pd crystal oriented in the (1, 1, 0) direction. Large spheres correspond to Pd atoms and the small dark sphere corresponds to an adsorbed hydrogen atom at site 2. Under-surface sites (site 3) and bulk diffusion sites (site 4) are also indicated. In the left side,  $a$  corresponds to the lattice parameter of the fcc structure and  $r$  is the metal covalent radius.

method to evaluate the absorption of hydrogen by different alloys of Pd. The shape of the hydrogen desorption curve might give us some indication of the different adsorption/absorption sites present in these systems. Kinetic analyses of the curve would give us information such as desorption energy and order of the desorption process, using a powerful method of analysis which we have developed [27].

Some prior work on the hydrogen–Pd system focused mainly on characterizing the surface states of hydrogen chemisorption on single crystals at low temperature, using TDS. No significant bulk hydrogen uptake by Pd occurs at temperatures below 200 K. Since we are interested in the dissolution of hydrogen into the bulk of metals which could impact the membrane applications, this work is focused on studies of hydrogen adsorption/absorption from Pd and its alloys occurring at temperatures above 300 K.

## 2. Experimental

### 2.1. THERMAL DESORPTION ANALYSES USING THE MASS SPECTROMETER

Samples of pure Pd or 5% Ru–Pd or 16% Ag–Pd foil with approximate dimensions of  $1.0 \times 1.0 \times 0.0025$  cm were cut from a larger piece of foil obtained from Johnson Matthey, Ltd. (except Ag–Pd), and mounted on the manipulator. The purity of the foils was 99.999%, the highest purity available from Johnson Matthey. The foils were spot-welded to two 0.09 cm in diameter 316 stainless steel wires which were clamped to 0.32 cm copper bars of a sample manipulator. The temperature of the samples was monitored by a 0.0127 cm in diameter chromel–alumel

thermocouple spot-welded to one face of the foils. The sample was resistively heated using a high-current ac power supply.

The manipulator was placed inside a modified system from AMETEK (Thermox Instruments Division, Pittsburgh, PA) designed for gas analysis. This instrument consists of a vacuum system mounted on a mobil cart which incorporates a Dycor quadrupole gas analyzer. The instrument was equipped with a Balzers 50  $\ell/s$  Turbomolecular pump backed with a Leybold Trivac S/D 1, 6 B mechanical pump.

A six-way cross placed in the vacuum system, allows us to include the sample manipulator, an Ar ion sputtering gun, the quadrupole mass spectrometer, a Varian variable leak valve and a glass view port on the available flanges. The base pressure of the system after outgassing stayed in the middle  $10^{-9}$  Torr. This system is described in detail elsewhere [28].

High purity gases (at least 99.999) from Matheson (AGA Chile) or Air Products and Chemicals, Inc. were used in all the experiments described in this work.

## 2.2. SURFACE ANALYSES

Surface cleanliness and surface elemental composition of the foils were monitored with Auger electron spectroscopy (AES) in an independent vacuum chamber with a base pressure of  $1 \times 10^{-9}$  Torr. AES analyses were performed with a cylindrical mirror analyzer (CMA) from Physical Electronics using 2 keV electrons,  $1 \times 10^{-6}$  A beam current and 2 V peak-to-peak modulation. The spectra were obtained scanning from a 15–1000 eV energy range. More details of this surface analysis system can be found elsewhere [25,29].

## 2.3. X-RAY DIFFRACTION

X-ray diffraction patterns of the foils were taken at room temperature with a Rigaku diffractometer. The diffraction patterns were obtained with a Cu X-ray tube and a two-circle goniometer in the usual  $\theta$ – $\theta$  geometry. The X-ray tube was operated at a 9 kW on a rotating Cu anode, generating mainly Cu  $K\alpha$  radiation of 8.05 keV (0.154 nm). The goniometer was advanced between  $5^\circ$  and  $140^\circ$  at  $0.02^\circ/s$  in the whole  $2\theta$  interval. The diffracted X-rays were detected with a solid state detector. The diffraction patterns did not show any significant background signal.

## 3. Results and discussion

### 3.1. HYDROGEN DESORPTION FROM PURE Pd AND Pd ALLOY FOILS

The foils were subjected to several cycles of flash desorption to 900 K, in vacuum, and Ar ion sputtering with the purpose of reducing C or S contamination

from the surface. This treatment was tested in an independent experiment where the surface of Pd and Ru–Pd was checked with AES after each step. Initially, the surface appeared enriched with S after heating but mild sputtering with Ar ions was sufficient to clean it up. The foils were then exposed to 100, 500 or 1000 L of H<sub>2</sub> at room temperature, to perform the desorption experiments (1 L = 10<sup>-6</sup> Torr s). After the desorption experiments, the surfaces of the Pd foils were also inspected with AES and this characterization revealed that the foil remained clean.

The foils were heated to 900 K, at 10 K/s, and the desorbing gas detected by the mass spectrometer. Typical spectra of hydrogen desorption from a piece of 1 × 1 cm of Pd, Ru–Pd and Ag–Pd foils after exposures of 1000 L are displayed in fig. 2. The intensities of the curves were normalized making the most intense part of the spectrum equal to 100% in order to facilitate comparisons.

A broad peak of hydrogen, with a maximum at about 650 K is detected for pure Pd and agrees well with the work reported by Ertl's group [11]. This peak was interpreted by Ertl as diffused hydrogen coming from the bulk. Ertl observed that the shape of the hydrogen desorption spectrum was similar for Pd(1, 1, 0) and Pd(1, 1, 1) single crystals, after exposures to 600 L. For smaller exposures (below 6 L) the dominant peak is surface adsorbed hydrogen.

For the case of Ru–Pd, two peaks of hydrogen desorption can be observed for the different exposures. The first peak is detected at about 440 K and the second peak at 600 K. These two desorption temperatures are significantly lower than the temperature at which hydrogen desorbs from pure Pd.

The case of Ag–Pd is more complicated. There are two hydrogen desorption peaks too, one at 440 K and a second around 700 K. The ratio between the first and second peak changes depending on the time interval between the end of exposure

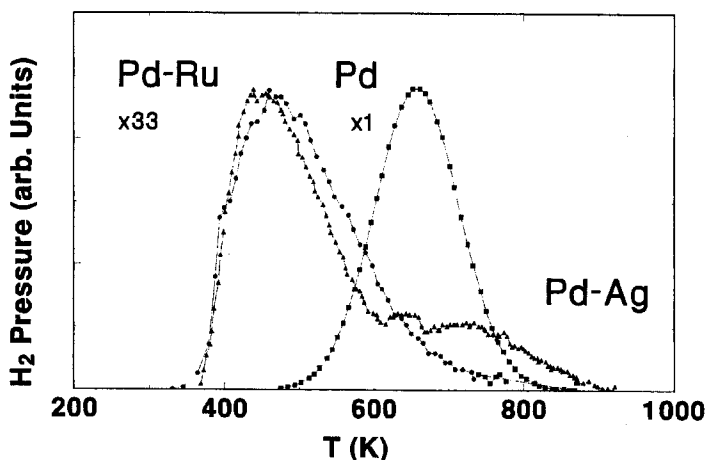


Fig. 2. TDS spectra for H<sub>2</sub> desorption from pure Pd, Ru–Pd and Ag–Pd foils after exposure to 1000 L of H<sub>2</sub> and using a heating rate of 10 K/s. The TDS curves for Ru–Pd and Ag–Pd are magnified 33 times.

time and the beginning of the sample heating. If the sample heating for the TDS begins right after the end of exposure time, the first peak is larger than the second peak. If the heating begins 0.5 h after the end of exposure time, its intensity decreases at the expense of an increase in intensity of the second peak. This is illustrated in fig. 3. The desorption curves can be deconvoluted into two peaks as illustrated in fig. 4 for the case of immediate desorption after 500 L of exposure from Ag-Pd.

Activation energy for desorption corresponding to a peak can be obtained by plotting the rate constant versus the inverse absolute temperature. The kinetic parameters are often coverage dependent and thus in our work they are only determined for the exposures under study.

The rate constant at each temperature point was obtained from the intensity value of the curve and the area integrated up to that temperature point. The basis of this type of analysis is given and explained in detail in a previous paper [27].

The rate constant ( $k$ ) is defined in the rate equation for desorption,

$$dN/dt = -kN^n, \quad (1)$$

where  $dN/dt$  is the rate of desorption,  $N$  is the concentration of adsorbed gas and  $n$  is the order of desorption. Since  $H_2$  molecules dissociate on the surface of transition metals, the order  $n$  taken as 2 in the analysis is plausible, but the order  $n$  is determined by the best fit of the data to a straight line in an Arrhenius plot. The rate constant  $k$  normally obeys an Arrhenius-type rate law of the form

$$k = v_n \exp(-E/RT), \quad (2)$$

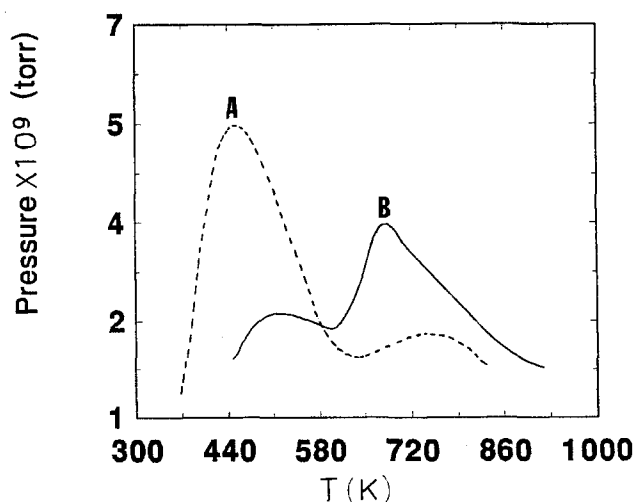


Fig. 3. TDS spectra for  $H_2$  desorption from Ag-Pd foil after exposure to 500 L of  $H_2$  and using a heating rate of 10 K/s: (A) Desorption performed immediately after exposure; (B) desorption performed 0.5 h after exposure to  $H_2$ .

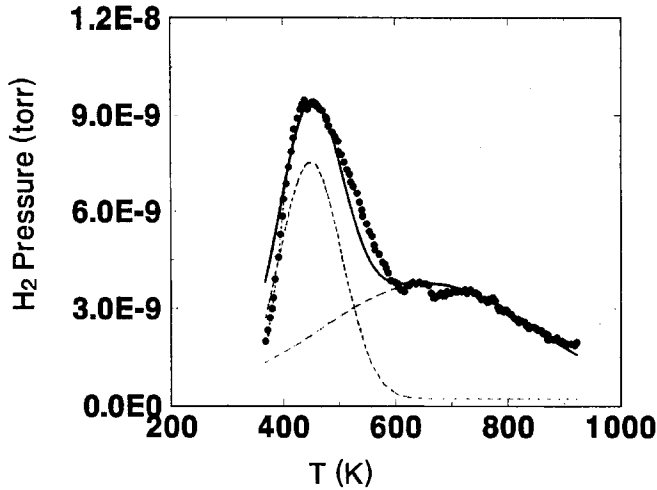


Fig. 4. Curve deconvolution of TDS shown in fig. 3, line A.

where  $v_n$  is the pre-exponential factor,  $R$  is the gas constant, and  $E$  is the activation energy. The constant  $k$  was evaluated from the desorption curve using the following relationship:

$$k = A_0^{n-1} B I(T) / [A_0 - A(T)]^n. \quad (3)$$

In eq. (3),  $A_0$  is the total area corresponding to one peak,  $B$  is the heating rate,  $I(T)$  is the value of the curve at the temperature  $T$ , and  $A(T)$  is the area under the curve up to the temperature  $T$ . The value of  $A_0$  is proportional to the “coverage” since it represents the initial concentration of atoms adsorbed for a given exposure.

The value of  $k$  was obtained from eq. (3) for each curve shown in fig. 2 assuming several desorption orders, the  $\ln(k)$  versus the inverse absolute temperature was plotted until a straight line was obtained.

For the high temperature peak, a straight line is obtained only with  $n = 1.25$  for all the cases. The slope of the Arrhenius lines yields activation energies corresponding to  $8.5 \pm 0.5$  kcal/mol for pure Pd,  $5.6 \pm 0.5$  kcal/mol for Ru–Pd and  $3.5 \pm 0.5$  kcal/mol for Ag–Pd. We attempted to fit the data with  $n = 1$  and  $n = 2$ , but the best fit was with a fractional number,  $n = 1.25$ . The energy value obtained is in agreement with various values reported in the literature for a weakly bound surface state [16,17]. The appearance of a fractional order for desorption was explained by Ertl [17] as a consequence of the fast replacement of the desorbing hydrogen atoms by atoms moving up from below the surface.

For the low temperature peak, a straight line is obtained with  $n = 2$  for all the cases. The slopes of the Arrhenius lines yield activation energies corresponding to  $10.7 \pm 0.5$  kcal/mol for Ru–Pd and  $8.5 \pm 0.5$  kcal/mol for Ag–Pd. The fact that the order of the desorption for the first peak was  $n = 2$  indicates that hydrogen is desorbing from a surface site.

### 3.2. X-RAY CHARACTERIZATION OF THE FOILS

The X-ray diffraction data obtained for the pure Pd and Pd alloys foils before and after the experiments suggest that the microstructure of the Pd and Ag–Pd foil changed but the microstructure of the Ru–Pd foil was unaltered.

Initially, all the foils are preferentially oriented in the (1, 1, 0) direction (with some components in the (1, 0, 0) and (3, 1, 1) directions). The Ag–Pd foil shows also a strong line corresponding to the (1, 0, 0) direction. After hydrogen absorption at room temperature and heating the foils up to 900 K in vacuum to perform desorption, the diffraction pattern of Ru–Pd is almost identical to the initial pattern. This is shown in figs. 5A and 5B.

In the case of Pd and Ag–Pd, the diffraction pattern of the foils is completely changed after hydrogen absorption and desorption. The X-ray patterns are very similar to the respective powder diffraction patterns indicating that preferential orientation was destroyed. The diffraction patterns of Ag–Pd foils are shown in figs. 6A and 6B.

A foil of pure Pd was subjected to heating only in vacuum without exposure to hydrogen. The diffraction pattern revealed that small changes occurred suggesting that the orientation disorder is strongly related to the absorption of hydrogen. Dif-

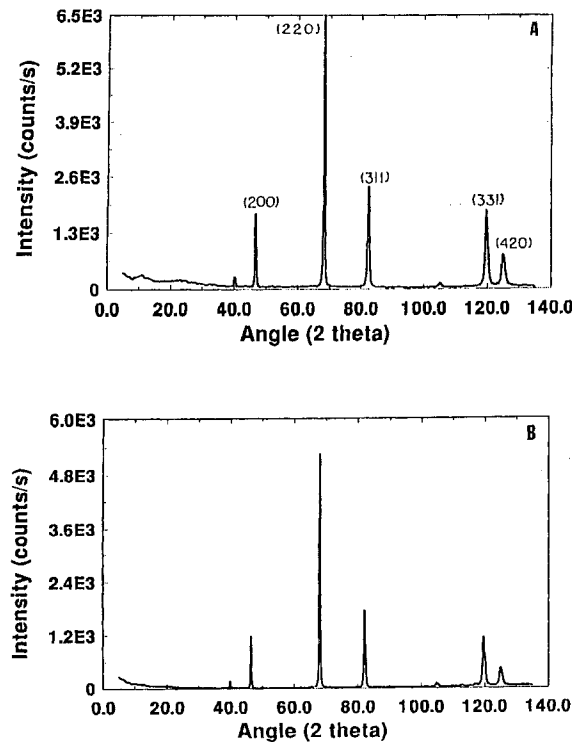


Fig. 5. X-ray diffraction pattern of Ru–Pd foil (A) without treatment and (B) after H<sub>2</sub> absorption.



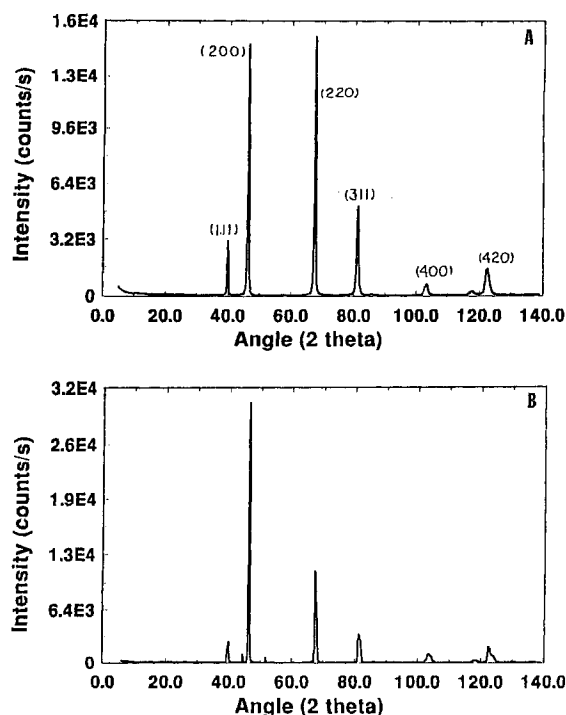


Fig. 6. X-ray diffraction pattern of Ag-Pd foil (A) without treatment and (B) after H<sub>2</sub> absorption.

fraction patterns illustrating this effect for pure Pd are shown in figs. 7A–7C. The lattice constants obtained from these diffraction patterns are listed in table 1.

The surface structure of Pd(1, 1, 0) represented in fig. 1 also shows the lattice parameter ( $a$ ), the metal covalent radius ( $r$ ) and the distance between opposite atoms in the unit cell ( $d$ ). In this figure, hydrogen and Pd atoms are drawn using their relative covalent radii. A hydrogen atom represented by the smaller dark circle is sitting at the surface in this figure. A hydrogen atom sitting at site 2 must be smaller than the distance  $d-4r$  in order to hop to one of the neighboring sites 3.

We have listed  $a$ ,  $d$ ,  $r$  and  $d-4r$  for Pd and its alloys in table 1. The lattice parameter ( $a$ ) was obtained from the XRD data presented in this work and the elemental covalent radius was obtained from the data base of the computer program (ref. [10]). As one can see from this calculations, the  $d-4r$  value is positive but very small for Pd, Ag-Pd and Ru-Pd alloys. The distance is larger for pure Pd and decreases in size for Ag-Pd and Ru-Pd, respectively. This is the same correlation observed for the amount of hydrogen absorbed by each of the samples, suggesting that crystallographic structure of the alloys is directly related to this absorption property.

Other elements are also listed in table 1. As one can see, the  $d-4r$  values are negative or very small for Ni, Cu and Ag, in agreement with the fact that these elements do not absorb hydrogen. This value is small but positive for Pt, suggesting that this might be a good candidate for hydrogen absorption.

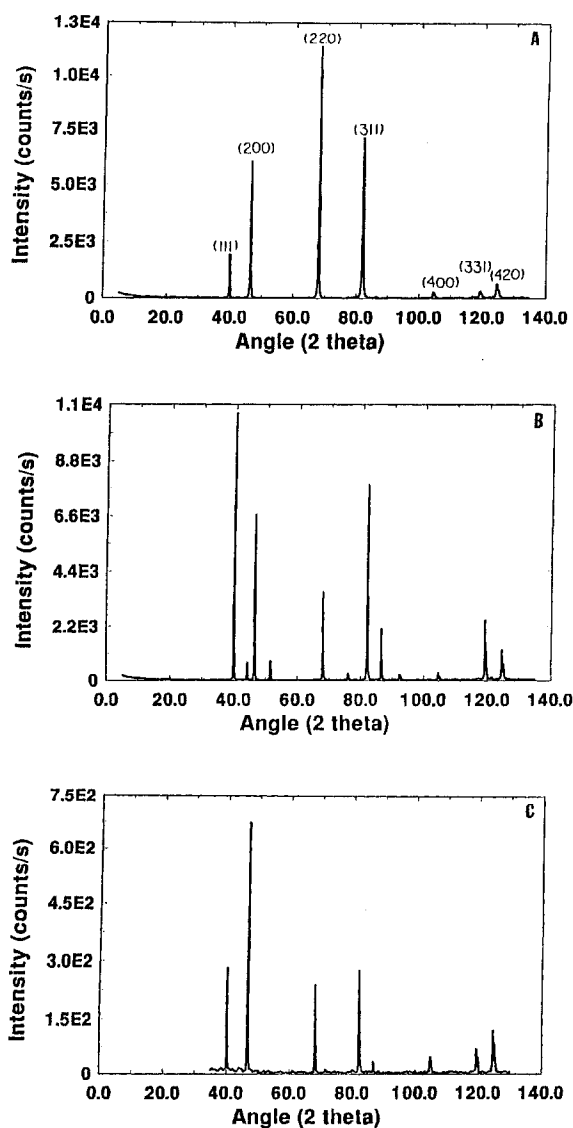


Fig. 7. X-ray diffraction pattern of pure Pd foil (A) without treatment, (B) after H<sub>2</sub> absorption and (C) after heating to 900 K in vacuum.

#### 4. Conclusions

One broad peak of hydrogen desorption at about 650 K is observed for Pd after exposure to hydrogen gas at 400 K. The absence of any other peak showing at lower temperatures indicates that the Pd surface is initially depleted of hydrogen at room temperature. Hydrogen adsorbed at the surface would desorb sooner than hydrogen absorbed in the bulk. In equilibrium, hydrogen would prefer to stay inside Pd rather than on the surface. The value of the desorption energy obtained in

Table 1  
Inter-atomic distances for Pd, Pd alloys and other fcc metals

Metal or alloy	$a$ (Å)	$d$ (Å)	$r$ (Å) <sup>a</sup>	$d-4r$ (Å)
<i>this work</i>				
Pd	3.895	5.5084	1.375	$8 \times 10^{-3}$
Ag-Pd	3.925	5.5508	1.386	$6 \times 10^{-3}$
Ru-Pd	3.892	5.5041	1.375	$4 \times 10^{-3}$
<i>literature values</i>				
Ag	4.086	5.779	1.445	$-1 \times 10^{-3}$
Ni	3.524	4.984	1.246	$-3 \times 10^{-4}$
Cu	3.615	5.112	1.278	$2 \times 10^{-7}$
Pt	3.924	5.549	1.387	$1 \times 10^{-3}$

<sup>a</sup> Literature value.

these experiments (8.5 kcal/mol) is larger than the energy for bulk diffusion (4.4 kcal/mol) and smaller than the energy of desorption from a surface chemisorbed state (20 kcal/mol, ref. [17]). These results agree well with the results of Behm et al. [17] using Pd(1, 1, 0) single crystals in which they found that the energy for this state was  $7 \pm 1$  kcal/mol.

A fractional order found for the desorption can be qualitatively explained with the argument given below. In the case of dissociative adsorption, the order can be  $n = 1$  if desorption proceeds from the recombination of immobile neighboring atoms. In principle, the order should be  $n = 2$  since there is some degree of surface diffusion before recombination. In this work, the surface hydrogen atoms are quickly replaced by atoms diffusing from the bulk, thus the surface hydrogen concentration always remains high during desorption. Therefore, for the most part, desorption proceeds by the recombination of two neighboring, immobile hydrogen atoms.

For the cases of the Ru-Pd and Ag-Pd alloys, two hydrogen peaks are observed under the same experimental conditions. We assume that the first peak corresponds to surface adsorption and the second peak to diffused hydrogen in the bulk. These results suggest that in equilibrium, hydrogen can occupy surface sites as well as penetrate into the bulk of the alloy. In Lagos' terminology, the energy for interstitial *absorption* is smaller than the energy for surface *adsorption*, and therefore some hydrogen atoms would prefer to be on the surface.

In fact, the energy of desorption from the assumed surface sites that we obtained from these experiments (10.7 kcal/mol for Ru-Pd and 8.5 kcal/mol for Ag-Pd) is larger than the energy for diffused hydrogen just below the surface (5.6 kcal/mol for Ru-Pd and 3.5 kcal/mol for Ag-Pd). These results are consistent with the fact that the energy of desorption from a reconstructed surface of Pd(1, 1, 0) decreases down to 12 kcal/mol [18], which might be caused by the effect of alloying Pd with small amounts of Ru or Ag.

These results suggest that 5% Ru-Pd is less effective than the Ag-Pd alloy and

this even less effective than pure Pd for the absorption and transport of hydrogen. We have determined by thermogravimetric analysis that alloying Pd with small quantities of Ru decreases the hydrogen solubility in the alloy by 20%, and, at the same time, changes the size of the interaction between hydrogen and metal atoms at the surface and near the surface.

One advantage of the Ru–Pd alloy over pure Pd is that it withstands more hydrogen absorption–desorption cycles, since the mechanical integrity of the foils is affected by the cycling between absorption–desorption and high–low temperature as indicated by prior reports [21] and our XRD data.

### Acknowledgement

Thanks are due to J.N. Armor (Air Products and Chemicals) for the initial motivation of this work and R.D. Penzhorn (Kernforschungszentrum Karlsruhe) for providing the Ag–Pd foil. This research was partially supported by grants from the Chilean Government (Fondecyt 1940696), Fundación Andes and US-Department of Energy. International travel was provided by CONYCIT and US NSF.

### References

- [1] V.M. Gryaznov, *Vestn. Akad. Nauk SSSR* (1986) 21.
- [2] V.M. Gryaznov, *Platinum Met. Rev.* 30 (1986) 68.
- [3] J. Shu, B.P.A. Grandjean, A. Van Neste and S. Kaliaguine, *Can. J. Chem. Engin.* 69 (1991) 1036.
- [4] M. Lagos, *Surf. Sci. Lett.* 122 (1982) L601.
- [5] M. Lagos and I.K. Schuller, *Surf. Sci.* 138 (1984) L161.
- [6] M. Lagos, G. Martinez and I.K. Schuller, *Phys. Rev. B* 29 (1985) 5979.
- [7] Y. Li, J.L. Erskine and A.C. Diebold, *Phys. Rev. B* 34 (1986) 5951.
- [8] K.H. Rieder and W. Stocker, *Phys. Rev. Lett.* 57 (1986) 2548.
- [9] K.H. Rieder, M. Baumberger and W. Stocker, *Phys. Rev. Lett.* 51 (1983) 1799.
- [10] M.A. Van Hove and K. Hermann, *Surface Architecture and Latuse*, a PC-based program, Version 2.0, Lawrence Berkeley Lab., Berkeley, LA, USA (1988).
- [11] H. Conrad, G. Ertl and E.E. Latta, *Surf. Sci.* 41 (1974) 435.
- [12] R.J. Behm, K. Christmann and G. Ertl, *Surf. Sci.* 99 (1980) 320.
- [13] M.G. Cattania, V. Penka, R.J. Behm, K. Christmann and G. Ertl, *Surf. Sci.* 126 (1983) 382.
- [14] C. Nyberg, L. Westerlund, L. Jonsson and S. Andersson, *J. Electron Spectry. Rel. Phenom.* 54/55 (1990) 639.
- [15] J-W. He and P.R. Norton, *Surf. Sci.* 195 (1988) L199.
- [16] J.F. Lynch and T.B. Flanagan, *J. Phys. Chem.* 77 (1973) 2628.
- [17] R.J. Behm, V. Penka, M.G. Cattania, K. Christmann and G. Ertl, *J. Chem. Phys.* 78 (1983) 7486.
- [18] G.E. Gdowski, T.E. Felter and R.H. Stulen, *Surf. Sci.* 181 (1987) L147.
- [19] W. Auer and H.J. Grabke, *Ber. Bunsenges. Physik. Chemie* 78 (1974) 58.
- [20] B.D. Kay, C.H.F. Peden and D.W. Goodman, *Phys. Rev. B* 34 (1986) 817.

- [21] J.N. Armor and T.S. Farris, in: *Proc. 10th Int. Congr. on Catalysis*, Budapest 1992 (Elsevier, Amsterdam, 1993).
- [22] R.J. Behm, K. Christmann, G. Ertl, M.A. Van Hove, P.A. Thiel and W.H. Weinberg, *Surf. Sci.* 88 (1979) L59.
- [23] R.J. Behm, K. Christmann, G. Ertl, M.A. Van Hove, *J. Chem. Phys.* 73 (1980) 2984.
- [24] A. Noordermeer, G.A. Kok and B.E. Nieuwenhuys, *Surf. Sci.* 165 (1986) 375.
- [25] A.L. Cabrera, *J. Vac. Sci. Technol. A* 8 (1990) 3229.
- [26] A.L. Cabrera, *J. Vac. Sci. Technol. A* 11 (1993) 205.
- [27] A.L. Cabrera, *J. Chem. Phys.* 93 (1990) 2854.
- [28] A.L. Cabrera, E. Morales, L. Altamirano and P. Espinoza, *Rev. Mex. Fis.* 39 (1993) 932.
- [29] A.L. Cabrera, N.D. Spencer, E. Kozak, P.W. Davis and G.A. Somorjai, *Rev. Sci. Instr.* 53 (1982) 1888.